

Extracting potential new targets for treatment of Adenoid Cystic Carcinoma using bioinformatic methods

Tayebeh Forooghi Pordanjani

Tarbiat Modares University Faculty of Biological Sciences

Bahareh Dabirmanesh

Tarbiat Modares University Faculty of Biological Sciences

Peyman Choopanian

Tarbiat Modares University Faculty of Basic Sciences

Mehdi Mirzaie

Tarbiat Modares University Faculty of Basic Sciences

Saleh Mohebbi

Iran University of Medical Sciences

Khosro Khajeh (✉ khajeh@modares.ac.ir)

Tarbiat Modares University Faculty of Biological Sciences

Research Article

Keywords: adenoid cystic carcinoma, biochemical pathway, protein interaction network, IGF1R, adipogenesis

Posted Date: July 6th, 2022

DOI: <https://doi.org/10.21203/rs.3.rs-783147/v2>

License: © ⓘ This work is licensed under a Creative Commons Attribution 4.0 International License.

[Read Full License](#)

Abstract

Adenoid cystic carcinoma (ACC) is a slow-growing malignancy that most often occurs in the salivary glands. Although reasonable local control is usually achieved by tumor surgery and subsequent radiation therapy, recurrence at the same or distant site is the cause of treatment failure. Currently, no FDA-approved therapeutic target or diagnostic biomarker has been identified for this cancer.

To find the therapeutic and diagnostic targets for ACC, we extracted the gene expression information from two GEO datasets. Different expression genes (DEGs) between ACC and normal samples were extracted and used to explore the biochemical pathways involved in ACC and create a protein-protein interaction (PPI) network.

After analyzing the PPI network, 20 hub genes were introduced that have potential as diagnostic and therapeutic target. Among them, *PLCG1* and *EZH2* were introduced as new biomarkers in ACC that might have a high value in the diagnosis and treatment of ACC. Furthermore, by studying the roles of the hub genes in the enriched biochemical pathways, we found that most likely, *IGF-1R/IR* and *PPARG* pathways play a critical role in tumorigenesis and drug resistance in the ACC and have a high potential for selection as a therapeutic target in future studies.

Introduction

About 40 types of salivary glands malignancy have been identified and distinguished by histology. Adenoid cystic carcinoma (ACC) is the most common neoplasm of the salivary glands after mucoepidermoid carcinoma. Diagnosis is currently performed by histological analysis of a biopsy or surgical sample. Differential diagnosis is made between ACC and other benign or malignant neoplasms in the same areas[1]. Despite the local control obtained after surgery of the primary tumor followed by radiation therapy, ACCs usually have a poor long-term prognosis[2]. More than 40% of ACC cases show distant metastasis. The lung, bone, and liver are the most common sites of metastasis[3]. ACC tends to spread along the craniofacial nerve trunk, which makes this tumor very destructive and unpredictable[4]. There is no chemotherapy available for patients with unresectable tumors[5]. Therefore, it is imperative to identify novel and effective biomarkers involved in tumorigenesis and drug resistance of ACC. To better understand the biochemical pathways involved in ACC pathogenesis, studying the signaling pathways using bioinformatics tools can be helpful. Molecular studies of ACC have been performed to determine the genomic sequence of patients and the expression profile of mRNAs involved in the disease.

Recent studies demonstrated that most ACC cases contain a translocation between chromosomes 6 and 9, which binds *MYB* proto-oncogene to the *NFIB* transcription factor locus or other enhancers and creates different fusion with *MYB*, followed by *MYB* overexpression[6],[1]. *MYB* protein is involved in regulating the transcription of many genes, including genes involved in the RNA processing, cell cycle, and DNA repair, thereby promotes tumor growth[7]. Since targeting transcription factors is complicated and there is still no drug to target *MYB*[8], it is necessary to identify applicable targets for ACC treatment by

understanding the mechanism of tumorigenesis. Although most ACC tumors show high MYB expression, it cannot be used as a biomarker to diagnose the disease because some specimens still show negative or poor staining[9]. MYB overexpression is also not specific to ACC and is seen in other tumors such as squamous cell carcinoma, which is confused with ACC[4]. Therefore, the aim of the present study was to unravel of dysregulated signaling pathways using bioinformatics and computational analysis to extract potential therapeutic and diagnostic targets.

One of the valuable tools for this goal is the analysis of data obtained from cDNA microarray with PPI network and enrichment analysis. In the present study, two original mRNA expression profiles were chosen from the GEO database. The DEGs between ACC and normal tissue samples were screened and used for Gene Ontology (GO), pathway enrichment analysis, and establishment of protein-protein interaction (PPI) network. Subsequently, 20 hub genes were identified. Evaluating the relationship between the enriched pathways and hub genes, revealed that inhibiting the IGF-II ligand and activating the PPARG pathway are two potential strategies against drug resistance in ACC. We also found a high correlation between MYB and PLCG1 expression for the first time. It seems that there is a link between PLCG1 and MYB oncogene. EZH2 is another hub gene that plays a critical role in tumorigenesis and is a valid therapeutic target in several tumors[10]. These results lead to new insights on drug target proteins in ACC for experimental biologists in the future.

Methods

Screening of Differential Expression Genes (DEGs)

We searched adenoid cystic carcinoma in the GEO database and then chose expression profile by array option. Two datasets, GSE59701 and GSE88804, were selected for the present analysis. The dataset GSE59701(submission year, 2015; year of last update, 2018) contains 12 ACC samples and 12 normal samples [11]. The dataset GSE88804(submission date, 2016; last update, 2018) contains 13 ACC samples and 7 normal samples [12]. The raw data of the mRNA expression profiles were downloaded as MINiML files. DEGs between ACC and normal samples in each dataset are extracted separately using the limma package in R software (version 3.6.0; <https://www.r-project.org/>). $|\logFC| > 1$ and adjusted P-value < 0.05 were set as the cut-off point which means the results are highly statistically significant. After extracting DEGs, the upregulated and downregulated genes in the two studies were collected and used for the subsequent analysis.

Go And Pathway Enrichment Analyses Of Degs

Enrichr, available at <http://amp.pharm.mssm.edu/Enrichr>, is a comprehensive web-based tool for gene set enrichment analysis[13]. Gene Ontology (GO) analysis, in the categories of molecular function, biological process, and cellular component were performed using Enrichr. In addition, the Kyoto Encyclopedia of Genes and Genomes (KEGG) pathway enrichment of DEGs, were performed to identify the signaling

pathways of the DEGs involved. We used all downregulated genes from two studies for finding downregulated pathways and used all upregulated genes for finding upregulated pathways from KEGG. Adjusted p-value < 0.05 was considered to cut-off criteria of statistical significance. We analyzed the enriched pathways, based on DEGs, to find out which axes in each pathway are dysregulated in the ACC samples compared to normal. Then we established the connection between the axes based on the KEGG data. Correlation between dysregulated pairs of KEGG pathways was obtained and demonstrated using a heat map.

Ppi Network Construction And Hub Genes Exploration

Before drawing the protein-protein interaction network, the overlapping DEGs were identified by Venn diagram (<http://bioinformatics.psb.ugent.be/webtools/Venn/>). We used 761 genes from upregulated and downregulated pathways to generate a PPI network using STRING database (<https://string-db.org>)[14]. After uploaded genes into the STRING website, the organism was set to Homosapiens, and the minimum required interaction score was set to medium confidence (0.4). PPI network data was exported in TSV format and import to Cytoscape software for visualization and analysis of the molecular interaction networks [15]. CytoHubba, a plugin tool in Cytoscape,[16] was applied to identify hub genes according to three topological analysis methods, including Edge percolated component(EPC), Maximum Neighborhood Component(MNC), and degree, and one centrality named Betweenness. To evaluate the diagnostic power of hub genes, a receiver operating characteristic (ROC) curve was generated using the pROC package in R software [17]. By calculating of the Area Under the Curve (AUC) for 20 hub genes, five genes with the highest AUC are plotted in a ROC curve.

Correlation Between The Expression Of Hub Genes And The Myb Oncogene

In order to investigate the relationship between the expression of 20 hub genes and MYB oncogene, the correlation coefficient of expression of hub genes with MYB was calculated and plotted in a Heat map. Red indicates a positive correlation, and blue indicates a negative correlation.

Results And Discussion

The two gene expression microarray datasets, GSE59701 and GSE88804, were obtained from GEO. Using the limma package in R software, a total of 2190 DEGs, including 1131 upregulated and 1059 downregulated genes, were obtained from two expression profile data (Table.1).

Table 1

Table 1
The number of upregulated and downregulated genes in ACC compared to normal tissue

references	GEO Accession number	Platform	Sample		DEG	
			ACC	normal	UP	DOWN
Gao R, et al. (2015)	GSE59701	GPL6244	12	12	696	496
Andersson MK.et al. (2017)	GSE88804	GPL6244	13	7	832	926
Total (Non-repetitive)			25	19	1131	1059

The GO analysis and KEGG signaling pathway enrichment of the 2190 DEGs were performed using the Enrichr database. We considered adjusted P value < 0.05 as the threshold to get meaningful pathways. Seventeen statistically significant pathways have been upregulated (Fig. 1). PI3K-Akt signaling pathway, Cell cycle, central carbon metabolism in cancer, focal adhesion, ECM receptor interaction, Wnt, axon guidance, microRNAs in cancer, and Ras signaling pathways are important pathways in ACC obtained from enrichment.

Results exhibited 33 downregulated pathways with the adjusted P value < 0.05 (Fig. 2). They can be divided into three groups. One group is related to salivary secretion. The second group is related to lipid metabolism and adipocyte differentiation including, the PPAR signaling pathway, AMPK, and adipocytokine signaling pathway. These three pathways show a high expression correlation in the heat map (Fig. 3). The third group is related to immune response and inflammation that cluster together in the heat map (Fig. 3). They include Rheumatoid Arthritis pathway, TNF signaling pathway, NOD-like receptor signaling pathway, NF-kappa B signaling pathway, IL-17 signaling pathway, and Phagosome.

Analysis of significant enriched pathways including PI3K-Akt, Ras, Wnt and, cell cycle that identified by Enrichr shed more light on the procedure of tumorigenesis of ACC. Figure 4 shows the upregulated axis in ACC. Protein interactions are based on KEGG pathways.

The PPI network of 761 overlapped DEGs was constructed using the STRING database and Cytoscape software (Fig. 5). Hub genes were obtained using the four mentioned methods separately. Thirty genes with the highest degree are shown in orange and yellow and others are shown in blue. Twenty of these genes were confirmed by three other methods of network analyses. They include TP53, EZH2, NOTCH1, CTNNB1, GNG2, APP, MET, KIT, PLCG1, LEF1, that are upregulated ones and BMP4, PPARG, IGF1, C3, CCL5, COX2, PRKCA, ERBB4, ADIPOQ, and, EGF are downregulated hub genes.

The substantial participation of some of the twenty hub genes, such as TP53[18], NOTCH1[19], CTNNB1[20], MET[5], and KIT[21] in the ACC tumorigenesis, has already been studied. The others need future studies to clarify their role in the ACC. The calculation of AUC for 20 hub genes was performed to validate their potential as a diagnostic biomarker (Fig. 6a). The CTNNB1, NOTCH1, PLCG1, PRKCA, and TP53 genes have an AUC of more than 0.98, indicating their high specificity and sensitivity in

distinguishing ACC samples from normal. Figure 6b shows the ROC curve for these five genes. To investigate the relationship between hub genes expression and MYB oncogene, the correlation between their expressions was calculated and shown by a heat map (Fig. 7). We found that in addition to TP53, CTNNB1, and NOTCH1, which have a decisive role in ACC[22],[23],[18], PLCG1 is a gene that its expression had a high correlation with MYB expression. This observation, together with the result obtained from the ROC curve propose this gene as a new diagnostic or therapeutic biomarker for future studies in ACC. A considerable role for PLCG1 in some cancers has been reported. In breast cancer, high expression of phosphorylated PLCG1 predicts metastasis in patients undergoing adjuvant chemotherapy[24]. In another study, PLCG1 inhibition induced programmed cell death in lung adenocarcinoma A549 cells[25].

EZH2 is another hub gene that appears to be particularly important in tumorigenesis. EZH2 participates in histone methylation of some tumor suppressor and inhibit them. The protein is only found in actively dividing cells [26], so it can be used as a diagnostic marker of dividing cells[27]. EZH2 can interact with Wnt signaling factors like MYC oncogene and cyclin D1 [28]. There is some FDA approve EZH2 inhibitors for treating different cancers[10]. Based on this evidence, investigation on EZH2 in ACC can be of great importance. In the following discussion, we will focus on the IGF-IR pathway and the PPARG pathway as two potential therapeutic pathways in ACC.

Genomic sequencing data, and cytogenetic maps revealed that most ACC cases have translocations that lead to the juxtaposition of *NFIB*, *TGFBR3* and *RAD51B* super-enhancers either upstream or downstream of *MYB* locus. MYB oncogene binds these translocated super-enhancers, loops to the *MYB* promoter, and cause positive feedback that increases itself expression[29],[11]. Increased MYB transcriptional regulatory activity promotes tumor cell proliferation in ACC by regulating genes involved in the RNA processing, cell cycle, and DNA repair highlighting MYB as a potential therapeutic target[4]. Interestingly, Andersson et al. found that IGF-1R /IR inhibition with linsitinib decreased the MYB-NFIB fusion product [2]. As a result, MYB–NFIB expression can be regulated by inhibiting the IGF1R pathway [2],[5]. However, the use of IR/IGF-IR inhibitors in the treatment of ACC was not very successful. Despite the use of these drugs inhibited tumor growth in xenografted ACC, but it did not affect cancer cell apoptosis[5]. Moreover, IGF-IR inhibition had a short-term clinical response, and the patient became resistant to treatment after a few months [2]. The reason for this drug resistance is the interaction of the IGF-1R pathway with other signaling pathways [30]. The IGF system has two ligands; IGF-1 and IGF-2, and three receptor; IGF-1R (primarily), IGF-2R, and the insulin receptor (IR), that IR itself has two variants named IR-B and IR-A[31]. According to DEGs analysis, IGF-2, IR and IGF-1R have been upregulated and IGF-1 has been downregulated in ACC. Similar to previous studies on the IGFIR-AKT axis in ACC [2], we found upregulation of PI3K-AKT signaling pathways in gene enrichment. Also, the analysis of the increased pathways obtained from KEGG showed the pivotal role of PI3K-AKT and RAS signaling pathways (Fig. 4), which are downstream pathways of IGF-IR/IR [32]. Mitogen signaling by IR has been described in some tumor models and several examples have been provided in which the IGF1R or IR compensates the inhibition of the opposite receptor[31]. Recent evidence has shown that many cancer cell types, including prostate, colorectal, breast, and lung cancers express not only the IGF1R but also the IR-A, the isoform with high affinity for both insulin and IGF-2 and is also associated with a poor prognosis[33]. By

activating IR-A, IGF-IR and IGF-1R/IR-A hybrid, IGF-2 can function as part of the drug resistance development system against IGF-1R inhibitors [31][34][35][36]. One solution is to study the effects of other IGFR/IR inhibitors[5]. However, IGF-1R/IR inhibitors cannot distinguish between IR-A and IR-B, and interfere with glucose metabolism leading to insulin resistance and hyperglycemia[30]. On the other hand, there is a link between hyperglycemia and cancer that may arise from preferential expression of IR-A[33]. IGF-II activates PI3K-Akt signaling in ACC through stimulation of IGF-IR and IR-A. One solution to these problems is to target IGF-II ligands directly. Because, in addition to have anti-proliferative activity, IGF-II inhibitors do not interfere with IR-B function. Dusigitumab (MEDI-573) is an IGF-1/IGF-2 co-neutralizing mAbs with a stronger binding affinity for IGF-2 than IGF-1. It has anti-proliferative activity in vitro and in vivo in preclinical models[37]. Therefore, IGF-2 could be a valuable new therapeutic target for ACC that has not been studied in ACC patients and requires future studies.

The second pathway that can be considered in ACC treatment is the PPARG pathway. Based on signaling pathway enrichment ACC's pathogenesis is mainly linked to lipid metabolism. Lipid metabolism signaling pathways including adipocyte signaling pathway, PPARG and AMPK have been downregulated in ACC. Figure 3 shows the high correlation of these pathways. Interestingly, there is a link between lipid metabolism and the IGF-1R pathway. IGF-1 promotes preadipocyte proliferation and differentiation, however IGF-IR abundance increase with adipocyte dedifferentiation[38]. IGF-2 has an inhibitory effect on the differentiation of visceral adipocytes that confirmed by reducing PPARG and ADIPOQ, two differentiation markers of adipocytes. Visceral adipocyte plays a substantial role in the pathogenicity of various diseases such as metabolic syndrome, type 2 diabetes, and cardiovascular risk[38]. IR-A is the predominant isoform in visceral preadipocytes and makes them more responsive to IGF-2. IR-B predominates in subcutaneous preadipocytes, so the binding of insulin to these cells has metabolic effects. Many types of tumors (breast, gastric, renal, colon, and ovarian) grow in the proximity of visceral adipocytes and induce dedifferentiation of visceral adipocytes into pre-adipocytes or reprogram them into cancer-associated adipocytes. Dedifferentiation of adipocytes causes the release of fatty acids into tumor microenvironment and supports the tumor growth [39]. If differentiation of these preadipocytes is induced again, the process of carcinogenesis may be prevented [40]. PPARG plays a critical role in adipocyte differentiation, insulin sensitization, lipid metabolism, and carcinogenesis[41]. PPARG pathway is strictly inhibited in ACC samples rather than normal samples (Fig. 2). We also found PPARG and ADIPOQ as hub genes in the PPI network. PPARG belongs to the nuclear hormone receptor superfamily named Peroxisome proliferator activated receptors (PPARs). Different PPAR pathways containing α , β , γ , and δ have been identified [39]. Only PPAR γ (PPARG) pathway has been inhibited in ACC. Several studies showed a significant reduction in PPARG expression in follicular thyroid cancer, esophageal cancer, cervical carcinoma, and colon cancer [41]. Activation of the PPARG pathway with its agonists may prevent tumor growth and proliferation by inhibition of PI3K and the Ras, downstream pathways of the Insulin/IGF axis [42]. Thiazolidinediones (TZD) are the most widely used synthetic agents bind to PPARG and activate it. After activation, PPARG moves to the nucleus and binds DNA to regulate the transcription of several genes, which ultimately increases the storage of fatty acids in adipocytes and differentiation of adipocytes. It also, reduces circulating fatty acids and improves insulin sensitivity[43] [44]. Ciglitazone, a

synthetic PPAR γ ligand, prevents the proliferation of A549 cells (human alveolar adenocarcinoma cells) [41]. PPAR γ activation by rosiglitazone and pioglitazone substantially induced apoptosis and cell cycle G2 arrest in bladder cancer cells [45]. Activated PPAR γ performs its inhibitory role in cell growth and proliferation by improving cell differentiation [46]. Although the connection between the PPAR γ and IGF pathways is not clearly recognized but, the therapeutic function of PPAR γ is observed in tumors which IGF pathway is upregulated [47]. In light of these pieces of evidence, PPAR γ agonists may be potentially preventive and therapeutic agents in ACC. In support of this hypothesis, there is a report that found metformin usage significantly improved DFS (Disease-Free Survival) in ACC [48]. The use of these drugs can complement the effect of TKI drugs in ACC. Interestingly the use of metformin in A549 cells reduced PLCG1 levels and induced autophagy[49], so there is a need for further research to uncover the effect of PPAR γ activating drugs in the treatment of ACC.

The third group of pathways that have decreased with a high correlation in the ACC (Fig. 3) were pathways related to inflammation and the immune system, which included TNF signaling pathway, NF-kappa B signaling pathway, NOD-like receptor signaling pathway, Rheumatoid arthritis pathway, phagosome, adipocytokine signaling pathway, and IL-17 signaling pathway. Although, the progression and invasion of cancer cells are mediated by proinflammatory factors in the tumor microenvironment, tumor-derived factors sometimes disrupt the host immune system, leading to anti-inflammatory conditions in the tumor microenvironment. This immunosuppressive situation is associated with tumor progression and poor prognosis for patients with advanced cancer[50]. Identifying the immune system inhibition process in the ACC and the role of immunosuppressive factors derived from tumor cells in disease progression provides new insights about ACC treatment through the host immune system activation.

Conclusion

In general, in this research, we extracted two new therapeutic targets for ACC treatment using bioinformatic tools and previous researches. Dysregulation of IGF-IR/PI3K/Akt axis in ACC due to the increase of IGF-II, plays a crucial role in tumorigenesis. So inhibition of IGF-II instead of IGF-IR/IR is suggested to avoid resistance to treatment and interference with glucose metabolism. Furthermore, inhibition of adipogenesis causes the release of fatty acids from adipocytes into the tumor microenvironment and helps tumor growth. Thus, activation of the PPAR γ pathway can reduce the available sources for tumor cells by differentiating adipocytes. Besides, from PPI network analysis of DEGs, we identified 20 hub genes including TP53, EZH2, NOTCH1, CTNNB1, GNG2, APP, MET, KIT, PLCG1, LEF1, BMP4, PPAR γ , ADIPOQ, IGF1, COX2, C3, CCL5, PRKCA, ERBB4, and EGF. Among them, EZH2 and PLCG1 have an essential role in tumorigenesis of other cancers and their roles in ACC have not yet been studied. PLCG1 expression has a high correlation coefficient with MYB. Moreover, it has the highest AUC score in the ROC curve. Further experimental studies are required to confirm the results of this study.

Declarations

Ethics approval

This is an observational study. The Tarbiat Modares University Research Ethics Committee has confirmed that no ethical approval is required.

Funding

The authors are grateful to the financial support by the Tarbiat Modares University.

Financial interests

The authors have no relevant financial or non-financial interests to disclose.

Author contribution

T.F.P. investigated and interpreted of data, wrote the article. B.D. revised the article, helped interpret the data. P.Ch. acquisition and analysis of data. M.M. designed the methodology. S.M. evaluated of research goals and aims. Kh.Kh. oversight and leadership responsibility for the research activity planning and execution. S.M. and Kh.Kh. reviewed and edited the manuscript. All authors contributed to the article and approved the submitted version.

Data availability

The datasets analysed during the current study are available in the GEO database (<https://www.ncbi.nlm.nih.gov/geo>) with GSE59701 and GSE88804 accession numbers.

References

1. Brill LB, Kanner WA, Fehr A et al (2011) Analysis of MYB expression and MYB-NFIB gene fusions in adenoid cystic carcinoma and other salivary neoplasms. *Mod Pathol* 24:1169–1176. <https://doi.org/10.1038/modpathol.2011.86>
2. Andersson MK, Aman P, Stenman G (2019) IGF2/IGF1R Signaling as a Therapeutic Target in MYB-Positive Adenoid Cystic Carcinomas and Other Fusion Gene-Driven Tumors. *cells* 1–15. <https://doi.org/10.3390/cells8080913>
3. Andreasen S (2018) Molecular features of adenoid cystic carcinoma with an emphasis on microRNA expression. PhD thesis. *Apmis* 126:7–57. <https://doi.org/10.1111/apm.12828>
4. Moskaluk CA (2013) Adenoid Cystic Carcinoma: Clinical and Molecular Features. *Head Neck Pathol* 7:17–22. <https://doi.org/10.1007/s12105-013-0426-3>
5. Andersson MK, Afshari MK, Andrén Y et al (2017) Targeting the Oncogenic Transcriptional Regulator MYB in Adenoid Cystic Carcinoma by Inhibition of IGF1R/AKT Signaling. *J Natl Cancer Inst* 109:1–10. <https://doi.org/10.1093/jnci/djx017>

6. Mitani Y, Rao PH, Futreal PA et al (2011) Novel chromosomal rearrangements and break points at the t(6;9) in salivary adenoid cystic carcinoma: Association with MYB-NFIB chimeric fusion, MYB expression, and clinical outcome. *Clin Cancer Res* 17:7003–7014. <https://doi.org/10.1158/1078-0432.CCR-11-1870>
7. Ferrarotto R, Heymach JV, Glisson BS (2016) MYB-fusions and other potential actionable targets in adenoid cystic carcinoma. *Curr Opin Oncol* 28:195–200. <https://doi.org/10.1097/CCO.0000000000000280>
8. Liu X, Xu Y, Han L, Yi Y (2018) Reassessing the Potential of Myb-targeted Anti-cancer Therapy. *J Cancer* 9:1259–1266. <https://doi.org/10.7150/jca.23992>
9. Mitani Y, Li J, Rao PH et al (2010) Comprehensive Analysis of the MYB-NFIB Gene Fusion in Salivary Adenoid Cystic Carcinoma: Incidence, Variability, and Clinicopathologic Significance Comprehensive Analysis of the MYB-NFIB Gene Fusion in Salivary Adenoid Cystic Carcinoma : Incidence, Va. <https://doi.org/10.1158/1078-0432.CCR-10-0463>
10. Duan R, Du W, Guo W (2020) EZH2: A novel target for cancer treatment. *J Hematol Oncol* 13:1–12. <https://doi.org/10.1186/s13045-020-00937-8>
11. Gao R, Cao C, Zhang M et al (2014) A unifying gene signature for adenoid cystic cancer identifies parallel MYB-dependent and MYB-independent therapeutic targets. *Oncotarget* 5. <https://doi.org/10.18632/oncotarget.2985>
12. Liu H, Huang G, Luo M Transcriptome analyses identify hub genes and potential mechanisms in adenoid cystic carcinoma
13. Kuleshov MV, Jones MR, Rouillard AD et al (2016) Enrichr: a comprehensive gene set enrichment analysis web server 2016 update. *Nucleic Acids Res* 44:W90–W97. <https://doi.org/10.1093/nar/gkw377>
14. Szklarczyk D, Gable AL, Lyon D et al (2019) STRING v11: protein–protein association networks with increased coverage, supporting functional discovery in genome-wide experimental datasets. *Nucleic Acids Res* 47:D607–D613. <https://doi.org/10.1093/nar/gky1131>
15. Shannon P, Markiel A, Ozier O et al (2003) Cytoscape: A Software Environment for Integrated Models of Biomolecular Interaction Networks. *Genome Res* 13:2498–2504. <https://doi.org/10.1101/gr.1239303>
16. Chin C, Chen S, Wu H et al (2014) cytoHubba: identifying hub objects and sub-networks from complex interactome. 8:1–7
17. Robin X, Turck N, Hainard A et al (2011) pROC: an open-source package for R and S + to analyze and compare ROC curves
18. Ferrarotto R, Mitani Y, Diao L et al (2017) Activating NOTCH1 Mutations Define a Distinct Subgroup of Patients With Adenoid Cystic Carcinoma Who Have Poor Prognosis, Propensity to Bone and Liver Metastasis, and Potential Responsiveness to Notch1 Inhibitors. *J Clin Oncol* 35:352–360. <https://doi.org/10.1200/JCO.2016.67.5264>

19. Zielinski R, Przytycki PF, Zheng J et al (2009) The crosstalk between EGF, IGF, and Insulin cell signaling pathways - computational and experimental analysis. 10:1–10. <https://doi.org/10.1186/1752-0509-3-88>
20. Park S, Vora M, Van Zante A et al (2020) Clinicopathologic implications of Myb and Beta-catenin expression in adenoid cystic carcinoma. *J Otolaryngol - Head Neck Surg* 49. <https://doi.org/10.1186/s40463-020-00446-1>
21. Tang Y, Liang X, Zheng M et al (2010) Expression of c-kit and Slug correlates with invasion and metastasis of salivary adenoid cystic carcinoma. *Oral Oncol* 46:311–316. <https://doi.org/10.1016/j.oraloncology.2010.02.001>
22. Li Q, Huang P, Zheng C et al (2017) Prognostic significance of p53 immunohistochemical expression in adenoid cystic carcinoma of the salivary glands: A metaanalysis. *Oncotarget* 8:29458–29473. <https://doi.org/10.18632/oncotarget.15297>
23. Cavalcante RB, Nonaka CFW, de Santos HB et al (2018) Assessment of CTNNB1 gene mutations and β -catenin immunoexpression in salivary gland pleomorphic adenomas and adenoid cystic carcinomas. *Virchows Arch* 472:999–1005. <https://doi.org/10.1007/s00428-018-2335-z>
24. Emmanouilidi A, Lattanzio R, Sala G et al (2017) The role of phospholipase C γ 1 in breast cancer and its clinical significance. *Futur Oncol* 13:1991–1997. <https://doi.org/10.2217/fon-2017-0125>
25. Lu X, Fu H, Chen R et al (2020) Phosphoinositide specific phospholipase C γ 1 inhibition- driven autophagy caused cell death in human lung adenocarcinoma A549 cells in vivo and in vitro. 16. <https://doi.org/10.7150/ijbs.42962>
26. Konze KD, Ma A, Li F et al (2013) An orally bioavailable chemical probe of the lysine methyltransferases EZH2 and EZH1. *ACS Chem Biol* 8:1324–1334. <https://doi.org/10.1021/cb400133j>
27. Li J, Hart RP, Mallimo EM et al (2013) EZH2-mediated H3K27 trimethylation mediates neurodegeneration in ataxia-telangiectasia. *Nat Neurosci* 16:1745–1753. <https://doi.org/10.1038/nn.3564>
28. Shi B, Liang J, Yang X et al (2007) Integration of Estrogen and Wnt Signaling Circuits by the Polycomb Group Protein EZH2 in Breast Cancer Cells. *Mol Cell Biol* 27:5105–5119. <https://doi.org/10.1128/mcb.00162-07>
29. Drier Y, Cotton MJ, Williamson KE et al (2016) An oncogenic MYB feedback loop drives alternate cell fates in adenoid cystic carcinoma. *Nat Genet* 48:265–272. <https://doi.org/10.1038/ng.3502>
30. Simpson A, Petnga W, Macaulay VM et al (2017) Insulin-Like Growth Factor (IGF) Pathway Targeting in Cancer: Role of the IGF Axis and Opportunities for Future Combination Studies. *Target Oncol* 12:571–597. <https://doi.org/10.1007/s11523-017-0514-5>
31. Denduluri SK, Idowu O, Wang Z et al (2015) Insulin-like growth factor (IGF) signaling intumorigenesis and the development of cancer drug resistance. *Genes Dis* 2:13–25
32. Siddle K (2011) Signalling by insulin and IGF receptors: Supporting acts and new players. *J Mol Endocrinol* 47:1–10

33. The Insulin Receptor Isoform Exon 11- (IR-A) in Cancer and Other Diseases: A Review. *Horm Metab Res* 35:778–785. <https://doi.org/10.1055/s-2004-814157>
34. Vella V, Milluzzo A, Scalisi NM et al (2018) Insulin Receptor Isoforms in Cancer. 1–20. <https://doi.org/10.3390/ijms19113615>
35. Biernacka K, Perks CM, Holly et al (2019) The Neglected Insulin: IGF-II, a Metabolic Regulator with Implications for Diabetes, Obesity, and Cancer. *Cells* 8:1207. <https://doi.org/10.3390/cells8101207>
36. Pollak M (2012) The insulin and insulin-like growth factor receptor family in neoplasia: An update. *Nat Rev Cancer* 12:159–169
37. Gao J, Chesebrough JW, Cartlidge SA et al (2011) Dual IGF-I / II – Neutralizing Antibody MEDI-573 Potently Inhibits IGF Signaling and Tumor Growth. <https://doi.org/10.1158/0008-5472.CAN-10-2274>
38. Alfares MN, Perks CM, Hamilton-shield JP, Holly JMP (2020) Insulin-like growth factor-II in adipocyte regulation: depot-specific actions suggest a potential role limiting excess visceral adiposity. 1098–1107. <https://doi.org/10.1152/ajpendo.00409.2017>
39. Nieman KM, Romero IL, Van Houten B, Lengyel E (2013) Adipose tissue and adipocytes support tumorigenesis and metastasis. *Biochim Biophys Acta - Mol Cell Biol Lipids* 1831:1533–1541. <https://doi.org/10.1016/j.bbalip.2013.02.010>
40. Li Y, Mao AS, Seo BR et al (2020) Compression-induced dedifferentiation of adipocytes promotes tumor progression. 1–14
41. Zhang Z, Xu Y, Xu Q, Hou Y (2013) PPAR γ against Tumors by Different Signaling Pathways. 598–601. <https://doi.org/10.1159/000355328>
42. Belfiore A, Genua M, Malaguarnera R (2009) PPAR- γ agonists and their effects on igf-i receptor signaling: Implications for cancer. *PPAR Res*. <https://doi.org/10.1155/2009/830501>
43. Greenfield JR, Chisholm DJ (2004) Thiazolidinediones - Mechanisms of action. *Aust Prescr* 27:67–70
44. Malaguarnera R, Belfiore A (2011) The insulin receptor: A new target for cancer therapy. *Front Endocrinol (Lausanne)* 2:1–16. <https://doi.org/10.3389/fendo.2011.00093>
45. Lv S, Wang W, Wang H et al (2019) PPAR γ activation serves as therapeutic strategy against bladder cancer via inhibiting PI3K-Akt signaling pathway. *BMC Cancer* 19:204. <https://doi.org/10.1186/s12885-019-5426-6>
46. Gou Q, Gong X, Jin J et al (2017) Peroxisome proliferator-activated receptors (PPARs) are potential drug targets for cancer therapy. *Oncotarget* 8:60704–60709. <https://doi.org/10.18632/oncotarget.19610>
47. Vella V, Nicolosi ML, Giuliano S et al (2017) PPAR- γ agonists as antineoplastic agents in cancers with dysregulated IGF axis. *Front Endocrinol (Lausanne)* 8. <https://doi.org/10.3389/fendo.2017.00031>
48. Guo Y, Yu T, Yang J et al (2015) Metformin inhibits salivary adenocarcinoma growth through cell cycle arrest and apoptosis. *Am J Cancer Res* 5:3600–3611

49. Lattanzio R, Piantelli M, Falasca M (2013) Advances in Biological Regulation Role of phospholipase C in cell invasion and metastasis. *Adv Biol Regul* 53:309–318.
<https://doi.org/10.1016/j.jbior.2013.07.006>
50. Thibodeau J, Bourgeois-Daigneault MC, Lapointe R (2012) Targeting the MHC Class II antigen presentation pathway in cancer immunotherapy. *Oncoimmunology* 1:908–916.
<https://doi.org/10.4161/onci.21205>

Figures

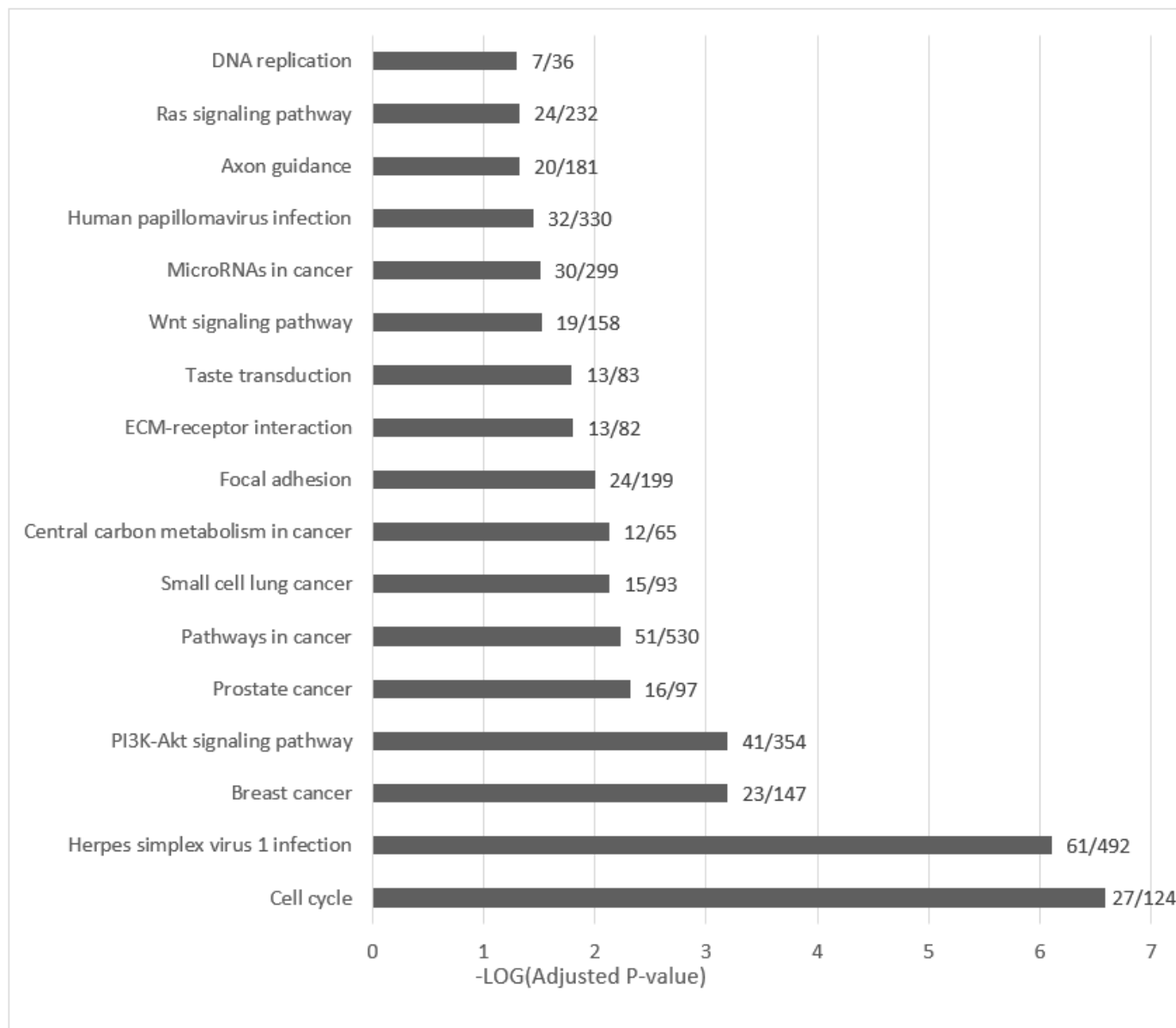


Figure 1

KEGG pathway enrichment analyses of upregulated DEGs in ACC samples vs. normal samples. Seventeen pathways have an adjusted p-value <0.05. The vertical axis represents the names of the

pathways. The horizontal axis represents the statistical significance that is calculated based on adjusted p-value. The numbers on the graphs indicate the number of genes changed in a pathway divided by the total number of genes in that pathway

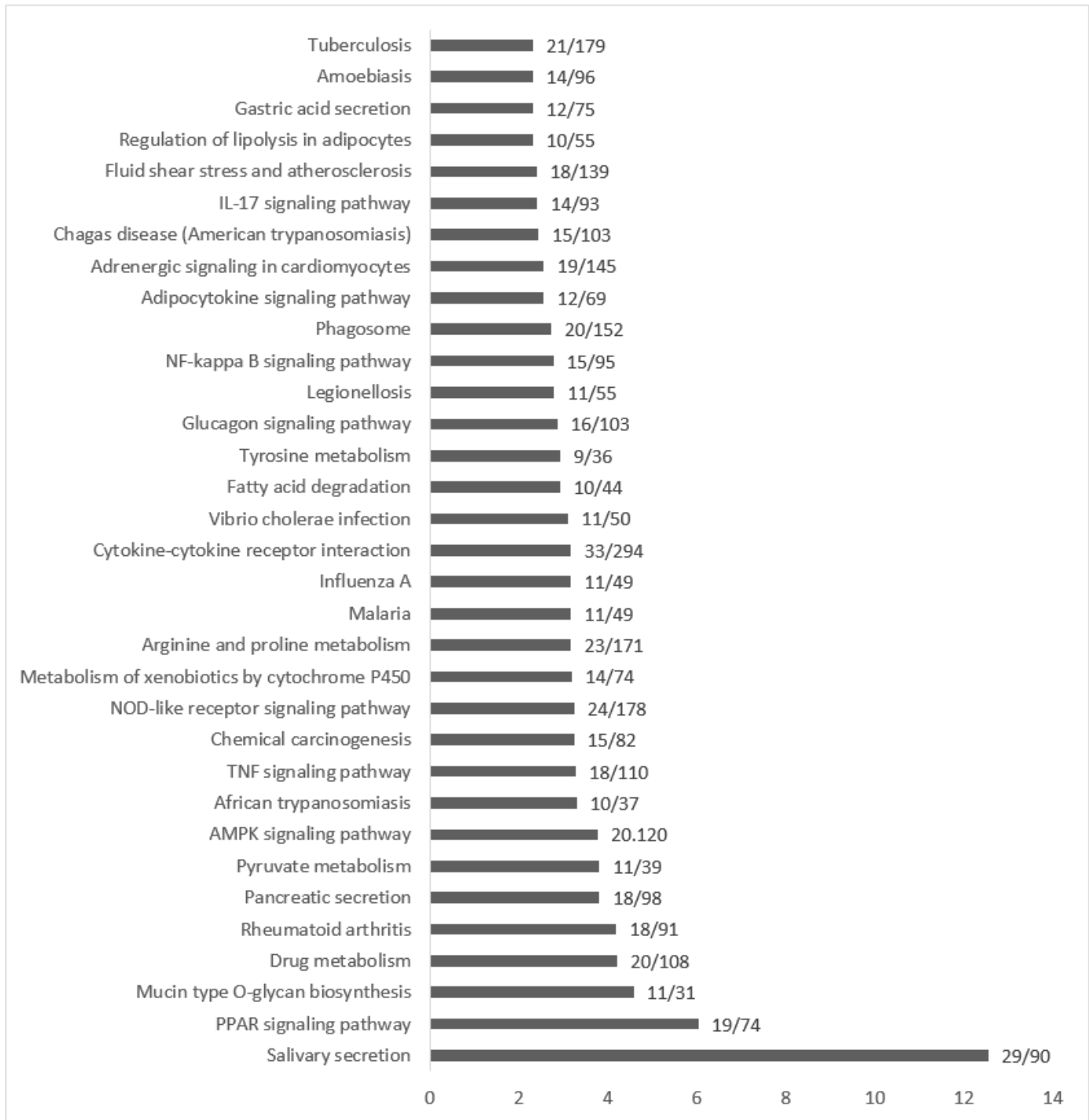


Figure 2

KEGG pathway enrichment analyses of downregulated DEGs in ACC samples vs. normal samples. Thirty-three pathways have an adjusted p-value <0.05. The vertical axis represents the names of the pathways. The horizontal axis represents the statistical significance that is calculated based on adjusted p-value.

The numbers on the graphs indicate the number of genes changed in a pathway divided by the total number of genes in that pathway

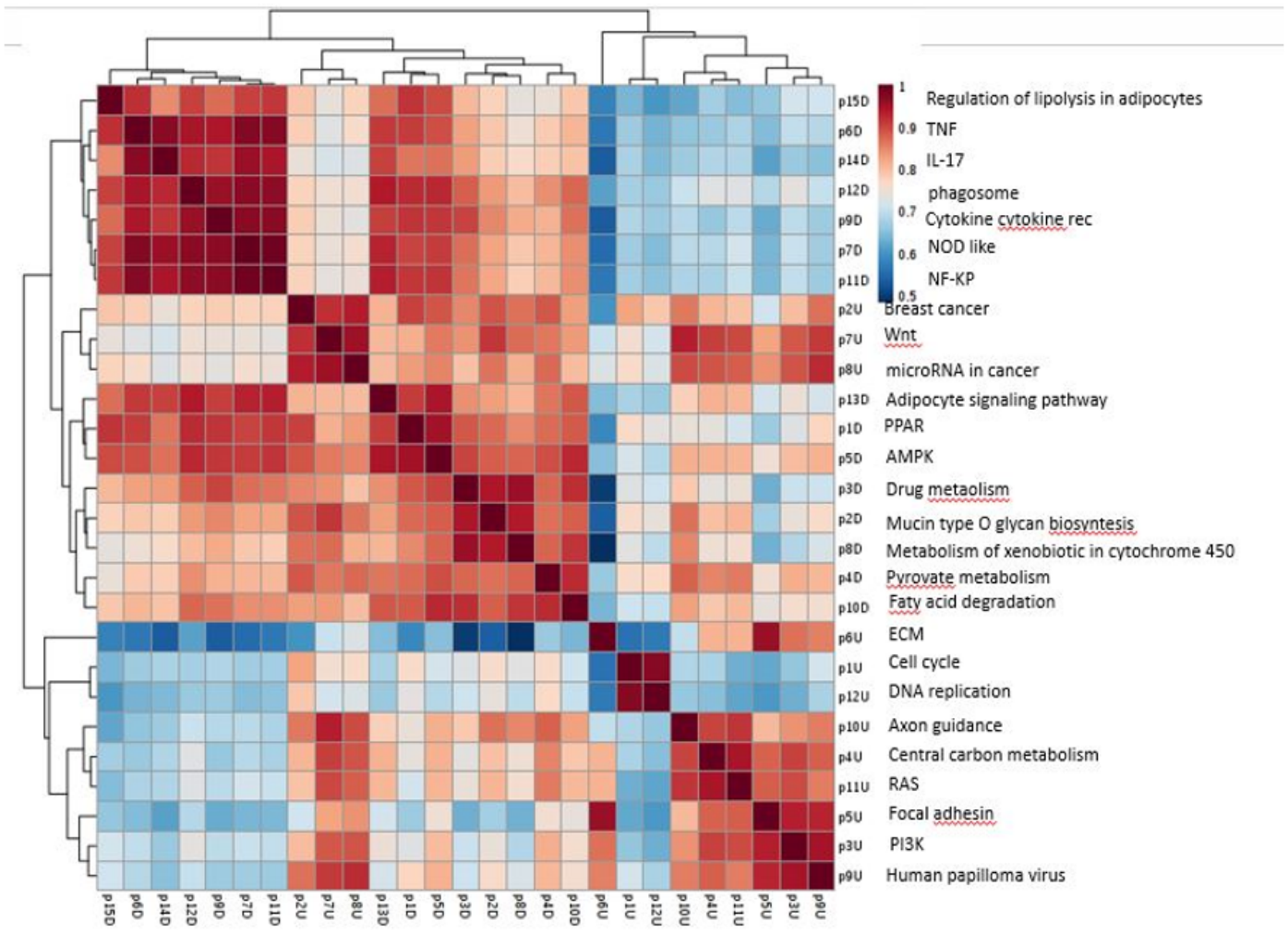


Figure 3

Heat map represents the correlation between the dysregulated pairs of KEGG pathways involved in ACC. Red indicates high correlation coefficients and blue indicates low correlation coefficients

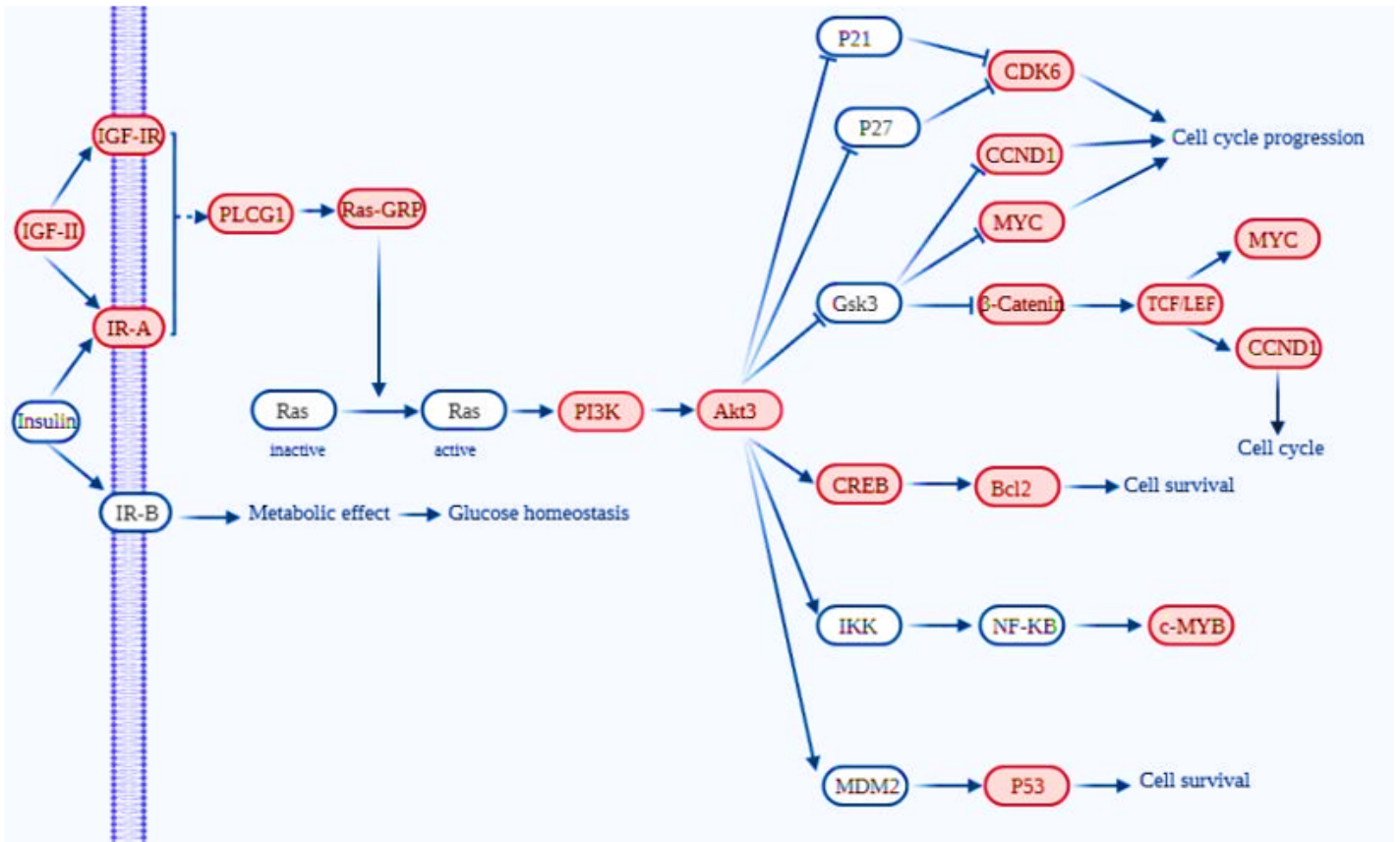


Figure 4

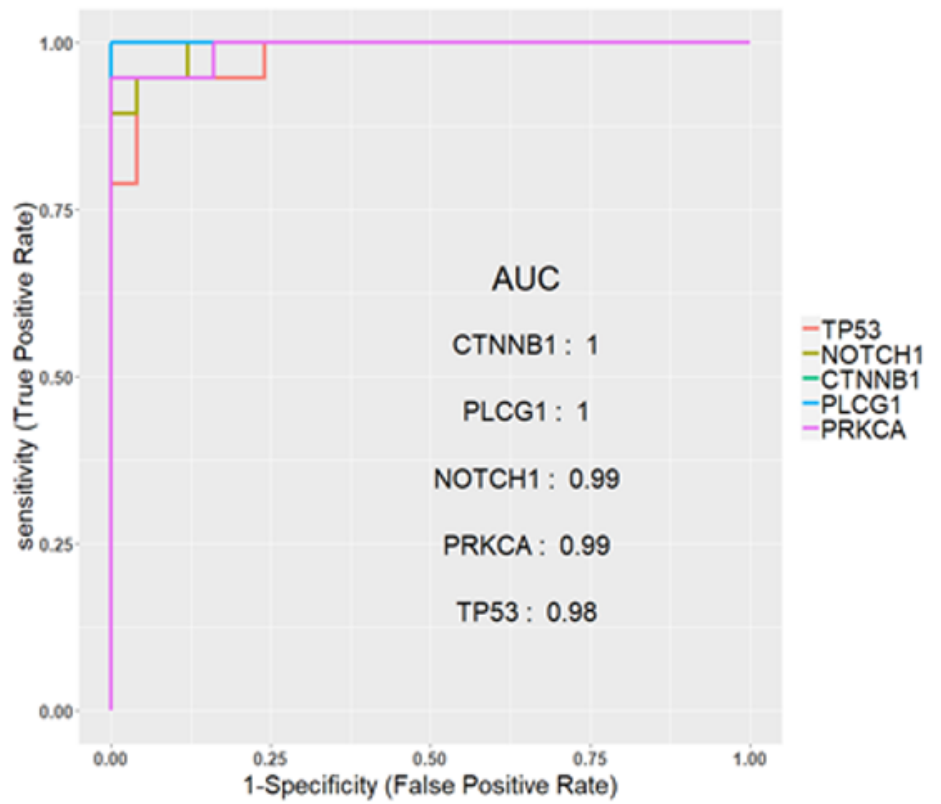
A simple schematic of the connection between the upregulated pathways in ACC, including IGF-1R/IR, RAS, PI3K/Akt, and Wnt based on KEGG pathways. Red indicates overexpressed genes according to DEGs

UBE2T	TAS2R10	CE51	TFAP2A	RASA1	GNB4	CDK6	GPC4	CTCF	PLXNB1	KDM5B	RGS2	LY96	SPDEF	IL2RG	EZH2	PRNP
PPARG	TEAD2	EFNA4	ACSL1	DLX5	EPHB3	GAS6	EPHA4	FBXO22	FZD7	CXCC5	RHOA	GREM2	NID1	RGCC	SLP1	RAB27B
DPYD	NOTCH1	LPAR3	TSC22D3	PLTP	MGLL	GLI3	SEMA6D	FGF10	UCP2	CDH11	OAS1	LOXL2	KLF15	FDCSP	SCRG1	DPF4
MMP16	ABCG1	MFG8	THBS2	ATP2A3	PTH2R	DLK1	ODAM	PRKCH	TESC	LPAR1	TSPAN8	EFNA5	BNIP3	RASSF5	CTSL	FBXL2
EYA1	KAT2B	EBF1	COL4A1	BHLHA15	BIRC3	JAG1	BCL2	BMP4	C3	PRLR	CD74	DDX58	IGF1	DOCK7	FZD3	BGN
DUSP1	DGKA	NRP2	MFAP2	LDLRAP1	FNDC1	CREB3L1	ERO1L	GNG2	ETV1	MAPK13	CENPJ	LAPTM4B	CPT1A	PLCB4	PRELP	CD79A
TP53	TLR3	AQP3	GALNT6	CYTH2	KLK11	ADIRF	LEF1	GLS	BRIP1	LYZ	BMPR1B	SMAD9	SERPINB1	VCAN	PIP	CCL5
PLLP	PDK4	NQO1	TFAP2C	PTGS2	APP	HBB	MAOB	NAPEPLD	EGF	PALMD	APEX1	SPARC	ELAVL2	MET	FAT1	RASGRP1
FOXO2	AQP1	EDA2R	MPDZ	KPNA2	NRCAM	TUBA1A	NTRK3	IQGAP2	TCEA3	IP6K2	WNT5A	ADIPOQ	KLF4	ARG2	KNTC1	APBA2
GPX2	PDE3B	NOS1	WDFY2	SLC9A3R1	SERPINE2	RNF128	HEY2	C8orf4	LIFR	HIST1H3I	PTX3	ANLN	ALDH1A1	ST8SIA1	TIA1	OAS2
DTL	FABP7	FABP4	STMN1	ANG	FKBP5	PIKFYVE	ACADL	ACKR4	CXCL17	IGF1R	COLEC12	BAMBI	FLNA	XPO1	LGR6	TAS2R3
RUNX1	WIF1	EFNA3	SIX1	FGFR1	CTNNB1	HELLS	GNA14	CDH13	DEFB1	TCF7L1	DAPK1	LAMB1	MCM7	CXCL2	SMOC2	NDRG1
MYOC	PLCG1	ICAM3	GLMN	ZFH4	HBEGF	LCN2	TACR1	CHAD	KREMEN1	AFAP1	CHRD1	MYO10	TAS2R4	GPR15	PIGR	NRG4
RRAGD	CLU	RIK3AP1	BPIFB2	FABP3	TAS2R5	AGR2	HPGD	PLAT	KIRREL	ABCA13	COL4A2	HLF	SCD	E2F5	KIT	NLGN1
MTHFD1L	ERRF1	KCNJ15	CCDC8	SHC4	PRKCA	ZFP36	APBB2	GABBR1	EPAS1	CA2	CD69	ITGA9	SLCO2A1	OLFM4	TRO	CTSC
IFIT1	MYB	LYVE1	EN1	LRRK2	PITX1	FYB	IRAK3	ERBB4	PTPRD	EDIL3	SERPINH1	WEE1	CYSLTR1	IL17RB	ST3GAL4	XBP1
SDC2	XRCC2	CFD	HAPLN1	PTN	CCL21	IGHV4-38-2	ANXA1	SCNN1A	IL33	SOX4	CA13	KALRN	BCL2L11	CPSF6	EPHA7	CALD1
HOMER2	AOX1	FAM20A	SEMA3A	PAX9	CD38	SPSB1	EPHA2	S100A1	FGL2	TAS2R13						

Figure 5

Protein-protein interaction network of overlapping DEGs between two datasets. Thirty genes with the highest degree are shown in orange and yellow and others are shown in blue

gene	auc
ADIPOQ	0.888421
APP	0.917895
BMP4	0.945263
C3	0.856842
CCL5	0.877895
CTNNB1	1
EGF	0.821053
ERBB4	0.888421
EZH2	0.957895
GNG2	0.873684
IGF1	0.909474
KIT	0.955789
LEF1	0.915789
MET	0.831579
NOTCH1	0.991579
PLCG1	1
PPARG	0.934737
PRKCA	0.991579
PTGS2	0.903158
TP53	0.981053



a

b

Figure 6

(a) AUC calculation for 20 hub genes. (b) The ROC curve of five genes with the highest AUC

